Journal of Non-Crystalline Solids 357 (2011) 2702–2707

Contents lists available at ScienceDirect

Journal of Non-Crystalline Solids

journal homepage: www.elsevier.com/locate/jnoncrysol

Computational and Raman studies of phospho-tellurite glasses as ultrabroad Raman gain media

Takenobu Suzuki [*], Teruo William Shiosaka, Shohei Miyoshi, Yasutake Ohishi

Research Center for Advanced Photon Technology, Toyota Technological Institute, 2-12-1, Hisakata, Tempaku-ku, Nagoya 468–8511, Japan

A R T I C L E I N F O

Available online 12 March 2011

Keywords:
Phospho-tellurite glass;
Raman mode;
Molecular orbital calculation

A B S T R A C T

Molecular orbital calculations of two phospho-tellurite model clusters were performed to clarify the origins of the Raman bands in the Stokes region of over 1000 cm^{-1} in phospho-tellurite glasses. The Raman bands could be attributed to two components of 900–1050 cm^{-1} of symmetrical stretching vibrations of PO_4 units and 1050–1200 cm^{-1} of anti-symmetrical stretching vibrations of PO_4 units. It was also clarified that the top of the valence band of phospho-tellurite glasses consists of the lone pair electrons in a TeO_{4+1} unit and the bottom of the conduction band of the glass consists of the antibonding hybrids of Te 5p and O 2p orbitals in the equatorial plane of a TeO_4 unit.

We have developed new phospho-tellurite glasses which have the Raman gain peak of 30 times as large as silica glass or the Raman gain bandwidth of more than 1200 cm^{-1}.

1. Introduction

Stimulated Raman scattering is one of the most extensively studied nonlinear optical phenomena applicable to optoelectronic devices such as fiber Raman amplifiers, fiber Raman lasers, microsphere Raman lasers [1], silicon Raman laser [2] and so on. Raman gain media are more advantageous than Rare-earth ions-doped media, since the Raman gain can be obtained at any wavelength depending on the available pump wavelength. In other words, a pump spectrum determines a gain spectrum. Such freedom of the Raman gain spectrum enables advanced devices such as multi-wavelength pumping broadband fiber Raman amplifiers [3] and cascaded Raman lasers [4]. In optical fiber telecommunication applications, a fiber itself can be used as a Raman gain medium, this idea is realized distributed gain Raman amplifiers [5] to compensate the loss of the fiber.

Presently, pure and doped silica glasses fibers are the major Raman gain media in the optical fiber telecommunications. However, these fibers have the low and narrow Raman gain spectra. Tellurite glasses are characterized not only by the high and broad Raman gain [6,7] but also the high linear and nonlinear refractive indices [8], wide optical transmission window [9] and good chemical durability [10]. Thus tellurite glasses are promising candidates as Raman gain media. The glass should have high thermal stability against crystallization to be drawn into fiber form. Thermal stability of tellurite glasses can be improved by the addition of heavy metal oxides such as BaO and SrO [11]. The addition of other oxides such as P_2O_5, WO_3, Nb_2O_5 and MoO_3 expands and flattens the Raman gain spectra of tellurite glasses [8,11–15]. In particular, the addition of P_2O_5 to tellurite glasses effectively expands the Raman spectrum extending to 1200 cm^{-1} [16–19]. Such Raman modes in phospho-tellurite glasses were supposed to be stretching modes of P—O, but the detailed origin is still ambiguous. In addition, it is also unclear why a sharp peak at about 1300 cm^{-1} was not observed for phospho-tellurite glasses [17], though such a sharp peak is found for phosphate [20] and P-doped silica glasses [21]. In this paper, we will attribute stretching modes of P—O in the Raman spectra of phospho-tellurite glasses by molecular orbital calculations of model clusters of phospho-tellurite and discuss the network structure around phosphorus in phospho-tellurite glasses. We will also report on that the Raman characteristics of phosphate rich phospho-tellurite glasses that reveal the broader and flatter Raman gain than conventional tellurite glasses.

2. Computational details

Phospho-tellurite network structure was represented by two different cluster models shown in Fig. 1. Both of the clusters have the composition of $Te_5PO_{18}H_{11}$. The composition of these clusters corresponds to that of $89TeO_2-11P_2O_5$ phospho-tellurite glass. The dangling oxygen atoms in the cluster models were terminated by hydrogen atoms. The hydrogen atoms were described by the 3-21G [22] basis function set and O, P and Te atoms were described by the LanL2DZ double zeta basis functions [23–26] with p and d polarization functions. The electron correlation and exchange effects are included using density functional theory (DFT) with the B3LYP functional [27–29].

---

[*] Corresponding author.
E-mail address: takenobu@toyota-ti.ac.jp (T. Suzuki).

0022-3093/$ – see front matter © 2011 Elsevier B.V. All rights reserved.
doi:10.1016/j.jnoncrysol.2011.02.040

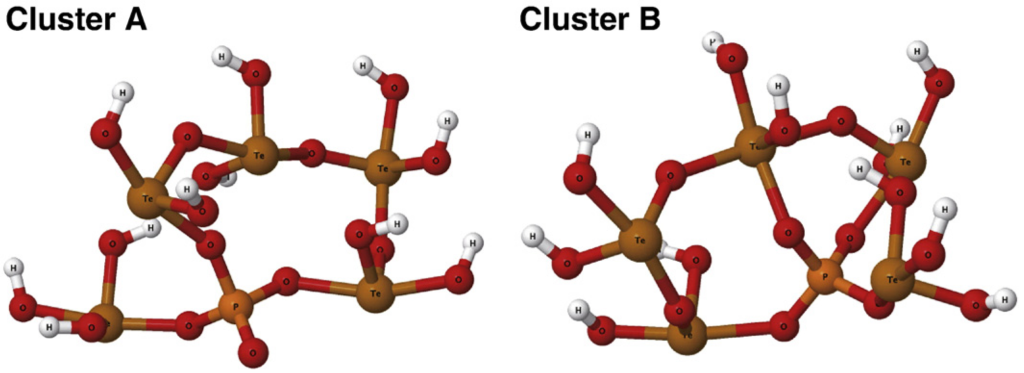

Fig. 1. Model clusters representing phospho-tellurite glass with a P═O double bond (Cluster A) and without a P═O double bond (Cluster B).

Full geometry optimization of clusters was performed within the C1 symmetry from different initial structures to obtain the final structures with and without a P O double bond. Vibrational frequency calculations were carried out using the optimized geometries. It was confirmed from the frequency calculations that the optimized structures were not saddle points but minima, since all the calculated vibrational frequencies were non-negative and the lowest frequencies of both models were $0 \pm 10\ \mathrm{cm}^{-1}$. The calculations have been performed using the Gaussian 03 [30] and GAMESS [31] *ab initio* molecular orbital calculation program packages.

3. Experimental

Changes in the Raman scattering characteristics of $(1-x)[80TeO_2$-$10Nb_2O_5$-$10MoO_3]$-$x[53.3P_2O_5$-$33.3SrO$-$13.3BaO]$ (in mol%) glasses were evaluated in this study. Glasses were prepared from high-purity TeO_2, Nb_2O_5, MoO_3, P_2O_5, $BaCO_3$ and $SrCO_3$ by a conventional melt-quenching technique.

Appropriate amounts of these chemicals were weighed and mixed in an alumina mortar and pestle inside a glove box in a nitrogen atmosphere. The mixed powders were melted in a platinum crucible at 900–1000 °C for 20 min by using an electrical furnace under N_2-O_2 gas flow atmosphere. The melt was then quenched onto a stainless steel plate, which was preheated at 350 °C, and the glass was subsequently annealed at the temperature for 10 h to release the thermal stresses developed during quenching. Annealed glasses were cut into rectangular pieces of 2 mm in thickness and polished well for optical measurements.

The refractive indices of the glasses were measured using a prism coupling method (Metricon, 2010) with lasers of wavelengths of 633, 974, 1320 and 1544 nm, at an accuracy better than ±0.001.

The spontaneous Raman spectra of bulk glass samples were measured with a Raman spectrometer (JASCO, model NRS 2100). The samples were excited using a CW-diode pumped-solid state laser (Coherent, Verdi) at the wavelength of 532 nm ($\tilde{\nu}_l = 1.880 \times 10^4\ \mathrm{cm}^{-1}$ in wavenumber) with a power of ≈500 mW. The Stokes Raman spectra were recorded in the range of 30–$1500\ \mathrm{cm}^{-1}$ in the back scattering alignment mode with co-polarization of incident and scattered light mode. The Raman spectrum of synthetic dry silica glass (ED-C, Tosoh) was also measured at the identical measurement conditions and used as an intensity standard. The observed Raman intensity of a glass was corrected for Fresnel reflection at the surface of the glass by the factor of F_R and for the change of solid angle of spatial distribution of scattered light by the factor of F_A [32]. F_R and F_A are given by

$$F_R(\tilde{\nu}) = \frac{[1+n_{sam}(\tilde{\nu}_l)]^2[1+n_{sam}(\tilde{\nu}_l-\tilde{\nu})]^2 n_{SiO_2}(\tilde{\nu}_l) n_{SiO_2}(\tilde{\nu}_l-\tilde{\nu})}{\left[1+n_{SiO_2}(\tilde{\nu}_l)\right]^2\left[1+n_{SiO_2}(\tilde{\nu}_l-\tilde{\nu})\right]^2 n_{sam}(\tilde{\nu}_l) n_{sam}(\tilde{\nu}_l-\tilde{\nu})} \quad (1)$$

and

$$F_A(\tilde{\nu}) = \frac{n_{sam}^2(\tilde{\nu}_l-\tilde{\nu})}{n_{SiO_2}^2(\tilde{\nu}_l-\tilde{\nu})} \quad (2)$$

where n_{sam} is the refractive index of the glass sample, n_{SiO_2} is the refractive index of the silica glass standard and $\tilde{\nu}$ is the Stokes shift in wavenumber. The Raman intensity should also be corrected by the Bose–Einstein distribution function, f_{BE} given by

$$f_{BE}(\tilde{\nu}, T) = \frac{1}{\exp\left(\frac{hc\tilde{\nu}}{k_B T}\right)-1} \quad (3)$$

where c is the speed of light in vacuum, h is Planck's constant, k_B is the Boltzmann constant and T is the temperature of Raman experiment. Thus the corrected intensity, I_{corr}, is obtained from the measured intensity, I_{meas}, by

$$I_{corr}(\tilde{\nu}) = I_{meas}(\tilde{\nu}) \cdot F_R(\tilde{\nu}) \cdot F_A(\tilde{\nu}) \cdot \frac{1}{f_{BE}(\tilde{\nu}, T)+1}. \quad (4)$$

The Raman gain coefficient spectra of glass samples were derived from the corrected spontaneous scattering intensity and by comparing with the gain coefficient spectrum of silica glass.

The Raman gain coefficient, g, is related to the spontaneous Raman scattering cross section as [33]

$$g(\tilde{\nu}) = \frac{\sigma(\tilde{\nu}) \cdot \left(\frac{1}{\tilde{\nu}_l-\tilde{\nu}}\right)^3}{c^2 \cdot h \cdot n^2(\nu_l-\tilde{\nu})} \quad (5)$$

where σ is the spontaneous Raman cross section. The reported value of the Raman gain coefficient of silica, $g_{SiO_2} = 1.86 \times 10^{13}$ m/W at a Stokes shift of $440\ \mathrm{cm}^{-1}$ for the 532 nm excitation [34] was used as the reference. The spontaneous Raman intensity of the sample was normalized to the corrected Raman intensity of silica at a peak of $\tilde{\nu}_p = 440\ \mathrm{cm}^{-1}$, $I_{corr,SiO_2}(\tilde{\nu}_p)$, as

$$I_{norm}(\tilde{\nu}) = I_{corr}(\tilde{\nu}) / I_{corr,SiO_2}\left(\tilde{\nu}_p\right). \quad (6)$$

σ is proportional to I_{norm} and can be written as $\sigma(\tilde{\nu}) = kI_{norm}(\tilde{\nu})$ where k is the proportional constant. k can be calculated from

$$k = g_{SiO_2} \cdot c^2 \cdot h \cdot n_{SiO_2}^2\left(\tilde{\nu}_l-\tilde{\nu}_p\right) \cdot \left(\tilde{\nu}_l-\tilde{\nu}_p\right)^3. \quad (7)$$